A novel modeling for performance assessment of kites as auxiliary propulsion device for merchant ships

A NOVEL MODELING FOR PERFORMANCE ASSESSMENT OF KITES AS AUXILIARY PROPULSION DEVICE FOR MERCHANT SHIPS

R Leloup, K Roncin, G Bles, J-B Leroux, C Jochum, LBMS (EA 4325), ENSTA - Bretagne, France, richard.leloup@ensta-bretagne.org, kostia.roncin@ensta-bretagne.fr, guilhem.bles@ensta-bretagne.fr, jean-baptiste.leroux@ensta-bretagne.fr, christian.jochum@ensta-bretagne.fr
Y Parlier, OCEA, rue des Terres Neuves, BP 21, 33322 Bègles Cedex, yves.parlier@parlier.org, **www.parlier.org**

SUMMARY

A performance prediction program dedicated to merchant ships was developed to assess fuel saving capabilities of a kite. The solving of the parameterization presented led to kite velocities and tethers tensions predictions continuously along a flight path within the wind window, including especially wind gradient and ship velocity. Both static and dynamic flight cases were considered regarding optimization strategy for kite tow efficiency. For dynamic flight case azimuth, elevation and orientation of the trajectory are continuously optimized in the present optimization algorithm. Finally, using a 320 m^2 kite on a 50 000 dwt tanker, the fuel saving computed is about 10 % for a wind velocity of 5 Beaufort and reaches more than 50 % for a wind velocity of 7 Beaufort.

NOMENCLATURE

Symbol	Definition	Unit
A_k	Kite surface	m^2
BSFC	brake specific fuel consumption	g.kWh^{-1}
C_D	Drag coefficient of the kite	[-]
C_L	Lift coefficient of the kite	[-]
$\mathbf{D}$	Kite drag vector	N
D	Kite drag magnitude	N
$\mathbf{F}_a$	Aerodynamic resultant vector	N
F_a	Aerodynamic resultant magnitude	N
F_{prop}	Force required from the ship propeller	N
J	Ship advance ratio	[-]
K_Q	Ship torque coefficient	[-]
K_T	Ship thrust coefficient	[-]
l_T	Tethers length	m
$\mathbf{L}$	Kite lift vector	N
L	Kite lift magnitude	N
n	is a coefficient which is equal to 1/7 for the sea surface according to ITTC 2011	[-]
n_{prop}	number of revolution per second of the ship propeller	Hz
P^*	Ship normalized brake power	[-]
P_B	Ship engine brake power	W
Q_p	Ship propeller torque	N.m
$\mathbf{T}$	Tethers tension vector	N
T	Tethers tension magnitude	N
T_{prop}	Ship required propeller thrust	N
$\mathbf{U}_{10}$	True wind velocity vector at standard altitude (10 m)	m.s^{-1}
U_{10}	True wind velocity magnitude at standard altitude (10 m)	m.s^{-1}
$\mathbf{V}_a$	Kite apparent wind velocity vector	m.s^{-1}
V_a	Kite apparent wind velocity magnitude	m.s^{-1}
V_A	advance velocity at the propeller	m.s^{-1}
$\mathbf{V}_k$	Kite velocity vector	m.s^{-1}
V_k	Kite velocity magnitude	m.s^{-1}
$\mathbf{V}_s$	Ship velocity vector	m.s^{-1}
V_s	Ship velocity magnitude	m.s^{-1}
$\mathbf{V}_{WR}$	Relative wind velocity at kite altitude (relative to boat course) vector	m.s^{-1}
V_{WR}	Relative wind velocity at kite altitude (relative to boat course) magnitude	m.s^{-1}
$\mathbf{V}_{WT}$	True wind velocity vector	m.s^{-1}
V_{WT}	True wind velocity magnitude	m.s^{-1}
z	Altitude above sea level	m
$\alpha_{geom.}$	Geometric incidence	rad
β_{WT}	True wind angle (relative to boat course)	rad
β_{WR}	Relative wind angle at kite altitude (relative to boat course)	rad
χ_{vk}	Cinematic azimuth	rad
ε	Kite lift to drag angle	rad
θ	Elevation angle	rad
ρ_{air}	Air density	kg.m^{-3}
ρ_{water}	Water density	kg.m^{-3}
ϕ	Azimuth angle	rad

Reference frames

R_a (K,$\mathbf{x}_a$,$\mathbf{y}_a$,$\mathbf{z}_a$)	Aerodynamic reference frame
R_F (K,$\mathbf{x}_F$,$\mathbf{y}_F$,$\mathbf{z}_F$)	Ship Velocity reference frame
R_{k0} (K,$\mathbf{x}_{k0}$,$\mathbf{y}_{k0}$,$\mathbf{z}_{k0}$)	Kite position reference frame
R_{WT} (O,$\mathbf{x}_{WT}$,$\mathbf{y}_{WT}$,$\mathbf{z}_{WT}$)	True wind reference frame
R_{WR} (A,$\mathbf{x}_{WR}$,$\mathbf{y}_{WR}$,$\mathbf{z}_{WR}$)	Relative wind at kite altitude reference frame
R_b (K,$\mathbf{x}_b$,$\mathbf{y}_b$,$\mathbf{z}_b$)	Body reference frame
$\mathbf{x}_{vk}$	Kite velocity direction unit vector

1. INTRODUCTION

It is well known today that the use of wind is one of the solutions to spare existing fossil energies. In this framework the IMO regulations concerning the reduction of emissions and the improvement of energy efficiency are putting the maritime industry in European seas under pressure. The study presented in this work takes place within the project "Beyond the Sea®" launched by Yves Parlier and is managed in partnership with the LBMS laboratory of ENSTA Bretagne and the French ministry of defence.

One of the first studies on kites and their ability to produce energy was achieved in 1980 [1]. More recently, the literature provides numerous articles which started to treat flight dynamics [2,3], flight control [4], structure deformation [5], or aerodynamic forces modelling [6,7].

Despite very fine approaches have been achieved in order to model the kite's flight applying Newton's laws [2,3,5], even taking into account kite's lines and mass distribution like de Goot [2], the so-called zero-mass model [8] remains well known and widely used as its simplicity makes it easy to connect with. Within this model, Newton's laws are applied considering only the aerodynamic resultant and tethers tensions, since the mass of the kite is neglected. For a given true wind velocity and position of the kite within the wind window, this leads to equations which can be solved explicitly for the unknown apparent wind velocity and tension in the lines [9].

Even recently, numerous studies dealing with flight strategies optimization for boat propulsion such as [8,10,11,12] or with real-time control for kites such as [13,14], rely on this kind of zero-mass approach. In fact, its very low computational cost and its reasonable predictions regarding experiments balance out its high level of approximation. As few examples it can be cited Wellicome [8] who compared stationary and dynamic flight strategies applying them for boat propulsion, Dadd et al. [15, 16] who studied dynamic flight with 8-shaped trajectories and obtained rather satisfactory comparisons with experimental measurements, Naaijen et al. [10,11] who developed a velocity prediction program dedicated to a merchant ship to assess fuel saving capabilities of a kite.

Regarding these last works, directly concerned with kites as auxiliary propulsion device for ships, each one proposed a kite trajectory optimization process in order to maximise the gain in propulsive force, for given wind conditions relative to ship courses. In their work, Naaijen et al. [10,11] limited the study to horizontal 8-shaped trajectories. They used a direct procedure to fix the elevation of the trajectory and finally only optimized its azimuth angle. On the other hand, Dadd [12] also introduced vertical 8-shaped trajectories and demonstrated that it enables significant benefits in upwind conditions. The Dadd optimization process consisted in choosing the best trajectory through a finite set of 10 predefined horizontal and vertical ones. In their studies, Naaijen et al. and Dadd took into account the wind gradient which results from the atmospheric boundary layer, but with some different levels of approximation.

Following these works, the aim of the present study is to optimize kite operation in each wind condition in a more general and continuous way. First, the modelling approach for a kite flying through the wind gradient linked to atmospheric boundary layer is presented. Especially, analytical expressions for apparent wind velocity seen by the kite and for kite velocity at each position within the wind window are detailed and taken into account.

Second, a parametrical definition of 8-shaped trajectories is introduced based either on Wellicome and Wilkinson [8] or Agatov et al. [17] works. This definition includes two parameters for the trajectory mean position in the wind window and a third extra one for its orientation, allowing continuous variations from horizontal to vertical flight paths. For each wind and ship conditions, those three parameters are processed continuously and simultaneously through a standard optimization algorithm, in order to get best flights configurations.

Third, the three modelling approaches and optimization techniques – Dadd [12], Naaijen et al. [10,11] and the one presented in this work – are compared on a case study documented by Dadd [12]. This leads to verifications of the present method, but also highlights its improvements. Finally, in the last section, the whole process is included in a velocity prediction program dedicated to a merchant ship, the *British Bombardier* studied by Naaijen et al. [10], which was developed to assess fuel saving capabilities of the kite. An illustration about fuel saving is given for the New-York to Cape Lizard route.

2. REFERENCE FRAMES

This section defines some reference frames that are essential in order to describe the placements and orientations of the kite and the true and relative winds within the wind window.

2.1 SHIP REFERENCE FRAMES.

As presented in figures 1 and 2, a moving ship is considered at a given velocity $\mathbf{V}_s$. In figure 2, O denotes the tether fastening point on the weather deck of the ship. Point A is vertical to point O at kite altitude. Point O is the origin of a reference frame called R_F. The orientation of reference frame R_F is fixed so that $\mathbf{x}_F$ axis is in the course direction along the ship velocity $\mathbf{V}_s$. We assume that the ship does neither roll nor pitch. Therefore, $\mathbf{z}_F$ is in the direction of the gravity acceleration.

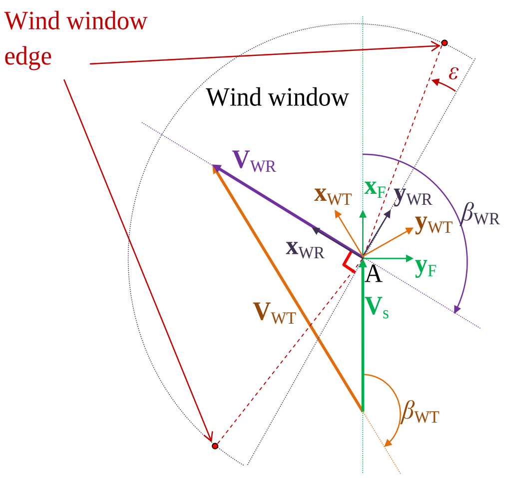

Figure 1: Wind window for an observer on the weather deck of a moving ship. The wind window orientation depends on the altitude over the sea. The diagram represents an horizontal plane at a given kite altitude.

Unit vector $\mathbf{x}_{WT}$ of the R_{WT} true wind reference frame is parallel to the true wind direction $\mathbf{V}_{WT}$. Therefore, R_{WT} corresponds to a rotation of reference frame R_F about vertical axis $\mathbf{z}_F$ of angle (β_{WT} - π). The orientation of relative wind reference frame R_{WR} is defined so that unit vector $\mathbf{x}_{WR}$ is parallel to the relative wind velocity $\mathbf{V}_{WR}$. Velocity $\mathbf{V}_{WR}$ depends on the kite altitude. Reference frame R_{WR} is the result of a rotation about axis $\mathbf{z}_F$ of angle (β_{WR} - π) applied to reference frame R_F. Angle β_{WR} is the relative wind angle (relative to boat course) and depends on kite altitude. The notation adopted here is the ITTC Standard notation [18] that allows, in the case of kite-boat, to distinguish the relative wind, which is experienced by the boat, from the apparent wind, which is experienced by the kite.

2.2 WIND WINDOW REFERENCE FRAMES.

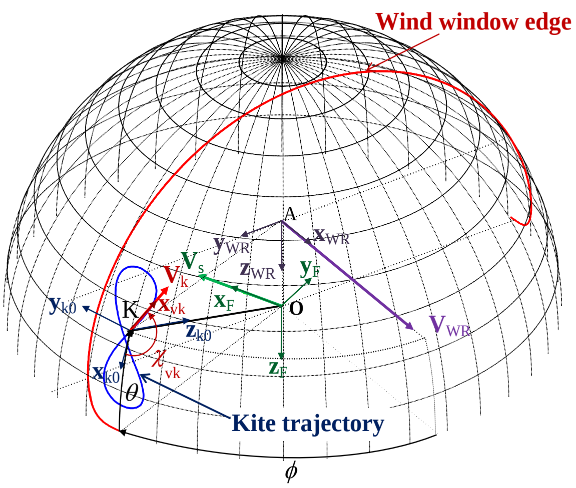

Figure 2: Flying kite within the wind window.

In case of a boat, the wind window orientation is defined by the relative wind velocity vector $\mathbf{V}_{WR}$ as shown in figure 2. Because of the wind gradient, the relative wind velocity field, experienced by the ship, is not uniform and depends on the altitude above the sea. Point K represents the kite; it is located in the symmetry plane of the kite and at the quarter chord as presented in figure 3. Point K is the origin of reference frame R_{k0}. The orientation of frame R_{k0} is obtained by two successive rotations applied to reference frame R_{WR}; a rotation of azimuth angle ϕ around axis $\mathbf{z}_{WR}$ and then a rotation of elevation angle (θ - π/2) about axis $\mathbf{y}_{k0}$. Vector $\mathbf{V}_k$ is the kite velocity. Unit vector $\mathbf{x}_{vk}$ corresponds to the direction of the kite velocity. Its orientation parameter is angle χ_{vk} within the tangent plane ($\mathbf{x}_{k0}$,$\mathbf{y}_{k0}$). Reference frame R_b is the body reference frame, attached to the kite. This frame rotates exactly like the kite. The origin of frame R_b is point K. Finally, the aerodynamic reference frame R_a is defined relating to the apparent wind velocity and the aerodynamic forces; unit vector $\mathbf{x}_a$ is parallel and opposite to the apparent wind velocity vector and drag force, while unit vector $\mathbf{z}_a$ is parallel and opposite to the lift force. We assume that the lift and drag forces are located in the kite symmetry plane.

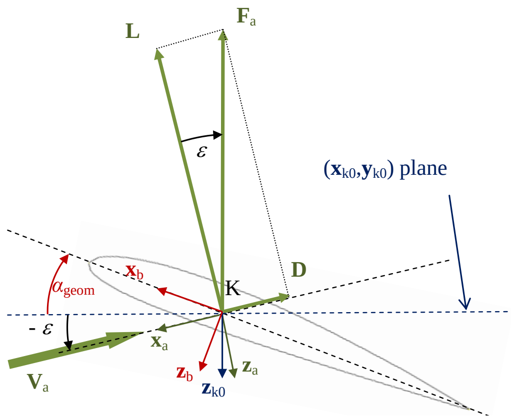

Figure 3: Aerodynamic forces vector decomposition in the kite symmetry plane.

3. MODELLING APPROACH OF A FLYING KITE BASED ON THE ZERO MASS ASSUMPTION

This section presents a review of the zero mass models [8,10,11,15,16], and these models are based on iterative algorithms. Therefore, a novel analytical expression is proposed in this study to enable a more time-efficient calculus of the velocity of the kite.

3.1 FUNDAMENTAL LAWS.

According to the Newton's laws applied to the kite at point K, and assuming that the mass of the kite is zero, we obtain:

$$\mathbf{T} + \mathbf{F}_a = \mathbf{0} \tag{1}$$

The aerodynamic resultant, $\mathbf{F}_a$, balances the tethers tension, $\mathbf{T}$, at any time and these two forces are aligned on the same axis that goes from attachment point O to the point K of the kite. The second equation which governs the kite motion is the apparent wind equation:

$$\mathbf{V}_{\mathrm{a}} = \mathbf{V}_{\mathrm{WR}} - \mathbf{V}_{\mathrm{k}} \tag{2}$$

With

$$\mathbf{V}_{\mathrm{WR}} = \mathbf{V}_{\mathrm{WT}} - \mathbf{V}_{\mathrm{s}} \tag{3}$$

Where, according to ITTC 2011 [18], the true wind velocity vector is:

$$\mathbf{V}_{\mathrm{WT}} = \mathbf{U}_{10} \left(\frac{z}{10}\right)^{n} \tag{4}$$

Where $\mathbf{U}_{10}$ is the wind velocity vector at standard altitude 10 m (m.s^{-1}),
z is altitude above sea level (m),
n is a coefficient which is equal to 1/7 regarding the sea surface considered by ITTC 2011 [18].

3.2 KITE VELOCITIES EXPRESSION IN THE ZERO-MASS MODEL FOR A MOVING KITE.

According to the definition of the aerodynamic resultant:

$$\mathbf{F}_{\mathrm{a}} = \mathbf{L} + \mathbf{D} \tag{5}$$

Where **L** is the lift and **D** the drag components of the aerodynamic force. By using the unit vectors shown in figure 3, this equation becomes:

$$- F_{\mathrm{a}}\, \mathbf{z}_{\mathrm{k0}} = - L\, \mathbf{z}_{\mathrm{a}} - D\, \mathbf{x}_{\mathrm{a}} \tag{6}$$

With

$$\begin{cases} L = \dfrac{1}{2}\rho_{\mathrm{air}} A_{\mathrm{k}} V_{\mathrm{a}}^{2} C_{\mathrm{L}} \\ D = \dfrac{1}{2}\rho_{\mathrm{air}} A_{\mathrm{k}} V_{\mathrm{a}}^{2} C_{\mathrm{D}} = L \tan \varepsilon \\ F_{\mathrm{a}} = \dfrac{L}{\cos \varepsilon} \end{cases} \tag{7}$$

Where ρ_{air} is air density,
A_{k} is kite surface,
C_{L} is the kite lift coefficient,
C_{D} is the kite drag coefficient,
ε is the kite lift to drag angle.

By definition of unit vectors $\mathbf{x}_{\mathrm{a}}$, $\mathbf{x}_{\mathrm{WR}}$ and $\mathbf{x}_{\mathrm{vk}}$, equation (2) becomes:

$$- V_{\mathrm{a}}\, \mathbf{x}_{\mathrm{a}} = V_{\mathrm{WR}}\, \mathbf{x}_{\mathrm{WR}} - V_{\mathrm{k}}\, \mathbf{x}_{\mathrm{vk}} \tag{8}$$

By scalar product of equation (8) with $\mathbf{z}_{\mathrm{k0}}$, we obtain:

$$V_{\mathrm{a}} = - \frac{V_{\mathrm{WR}}\, \mathbf{x}_{\mathrm{WR}}.\mathbf{z}_{\mathrm{k0}}}{\sin \varepsilon} \tag{9}$$

Moreover, using the scalar product properties, equation (2) leads to:

$$|\mathbf{V}_{\mathrm{a}}|^{2} = |\mathbf{V}_{\mathrm{WR}}|^{2} + |\mathbf{V}_{\mathrm{k}}|^{2} - 2\, |\mathbf{V}_{\mathrm{WR}}|\, |\mathbf{V}_{\mathrm{k}}|\, (\mathbf{x}_{\mathrm{WR}}.\mathbf{x}_{\mathrm{vk}}) \tag{10}$$

In the R_{WR} reference frame equation (9) combined with equation (10) can be seen as a second order equation of the velocity of the kite V_{k} leading therefore to:

$$V_{\mathrm{k}} = V_{\mathrm{WR}} \left[\mathbf{x}_{\mathrm{WR}}.\mathbf{x}_{\mathrm{vk}} + \sqrt{(\mathbf{x}_{\mathrm{WR}}.\mathbf{x}_{\mathrm{vk}})^{2} + \left(\frac{\mathbf{x}_{\mathrm{WR}}.\mathbf{z}_{\mathrm{k0}}}{\sin \varepsilon}\right)^{2} - 1} \right] \tag{11}$$

The negative solution of equation (10) corresponds to the positive solution for an angle $\pi + \chi_{\mathrm{vk}}$. Consequently, only the solution given by equation (11) is retained to agree with angle χ_{vk}.
The velocity of the kite is a real number only if

$$|\mathbf{x}_{\mathrm{WR}}.\mathbf{x}_{\mathrm{vk}}| \geq \sqrt{\left| 1 - \left(\frac{\mathbf{x}_{\mathrm{WR}}.\mathbf{z}_{\mathrm{k0}}}{\sin \varepsilon}\right)^{2} \right|} \tag{12}$$

Condition (12) shows that the existence of the velocity of the kite is only defined for a given flying area so-called manoeuvrable area below the red limit line shown in figure 2. In this area the kite can move in all directions. Above the red limit line, the kite cannot fly. It corresponds to the wind window edge.

3.3 STATIC FLIGHT PERFORMANCE.

Static flight can be described by zero kite velocity $\mathbf{V}_{\mathrm{k}}$ in equations (1) and (2). Apparent wind velocity $\mathbf{V}_{\mathrm{a}}$ is then equal to the relative wind velocity $\mathbf{V}_{\mathrm{WR}}$ experienced by the ship. According to the parameter notation presented in figure 2, solving the equations (1) and (2) leads to the following condition for kite positioning in the wind window:

$$\cos \phi = \pm \frac{\sin \varepsilon}{\cos \theta} \tag{1}$$

Azimuth angle ϕ is a function of elevation angle θ, which means that all possible positions of the kite during a static flight are located on a line that describes the wind window edge as shown in figure 2.

3.4 PROPULSIVE FORCE GENERATED BY THE KITE.

Once apparent wind velocity of the kite $\mathbf{V}_{\mathrm{a}}$ is known at each position within the wind window, the tethers tension resultant **T**, which is opposite to the aerodynamic resultant $\mathbf{F}_{\mathrm{a}}$ according to equation (1), can be expressed as follows:

$$\mathbf{T} = \frac{1}{2} \frac{C_{\mathrm{L}}\, \rho_{\mathrm{air}}\, A_{\mathrm{k}}\, V_{\mathrm{a}}^{2}}{\cos \varepsilon}\, \mathbf{z}_{\mathrm{k0}} \tag{14}$$

The projection of the tethers tension onto axis $\mathbf{x}_{\mathrm{F}}$, directly gives the propulsive force generated by the kite at a given position in the wind window. It depends on the relative wind angle β_{WR} at kite altitude as presented in figure 1. Projecting onto axis $\mathbf{y}_{\mathrm{F}}$, we obtain the drift force. These forces are integrated with respect to time along the flight trajectory of the kite, in order to obtain their average values for a given trajectory. This enables comparison between dynamic and static flight efficiency based on average propulsive force.

4. DYNAMIC FLIGHT TRAJECTORY OPTIMIZATION

4.1 INITIAL DATA

For a given vessel speed $\mathbf{V}_s$, and a given true wind direction β_{WR} and velocity $\mathbf{V}_{WR}$, control parameters for both static and dynamic flights are optimized. Especially, in case of a dynamic flight, resulting average propulsive force, as defined in paragraph 3.4, was considered to assess the efficiency of a trajectory. The most common trajectory applied to kite flights is the so-called 8-shaped trajectory, which avoids tethers to get tangled. The most commonly used mathematical expression of an 8-shaped trajectory is given by Argatov et al. [17] and Wellicome and Wilkinson [8]. Argatov et al. trajectory definition is much simpler than Wellicome and Wilkinson trajectory despite Wellicome and Wilkinson definition allows dissymmetrical trajectories. For the same trajectory size (azimuth and elevation amplitude), the difference in average propulsive forces obtained with the two trajectory definitions is about 0.15 %. The improvement of trajectory efficiency within the wind window can be done by acting on following parameters, as shown in figure 4:

- The shape of the trajectory,
  - Azimuth amplitude
  - Elevation amplitude
- The positioning in the wind window,
  - Elevation of the centre of the trajectory
  - Azimuth of the centre of the trajectory
- The trajectory orientation (rotation about $\mathbf{z}_{k0}$ axis).

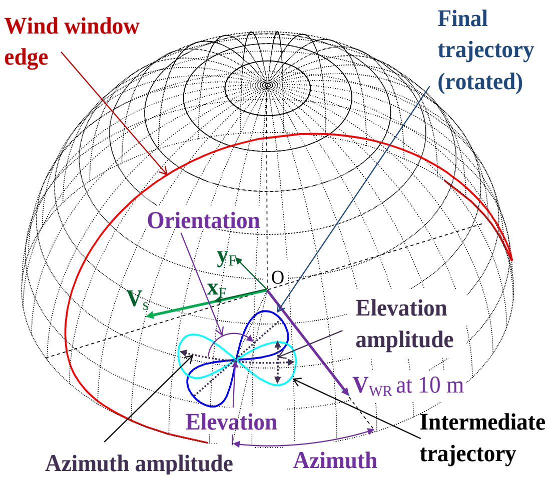

Figure 4: Trajectory parameters in the wind windows.

4.2 SHAPE OF THE TRAJECTORY

The shape of the trajectory can be modified thanks to azimuth and elevation amplitude parameters [8,17]. In the scope of the zero-mass model assumptions, the trajectory size reduction (azimuth and elevation amplitude decrease) enhances trajectory efficiency from a propulsive force point of view [8,16]. Dadd used large trajectories because he explains that “[…] the practical minimum limits for these are not known” [12]. Therefore, the same trajectory size as Dadd’s case study was retained.

4.3 WIND WINDOW POSITIONING AND ORIENTATION

Kite efficiency improvement could be performed by a better positioning of the trajectory in the wind window, thanks to azimuth and elevation settings.

The propulsive force is provided by the projection of the tether forces onto the vessel motion direction $\mathbf{x}_F$, as defined in paragraph 3.4. A closer direction of the tethers with the ship course results in a more efficient orientation of the kite developed forces (i.e. decrease of angle $\pi - \phi - \beta_{WR}$ angle, as illustrated in figures 1 and 2).

If the tether tension projection onto vessel axis is negative, it denotes a negative propulsive force. Thus, useful wind window would be smaller as relative wind angle β_{WR} decreases as shown in figure 5. On the other hand, maximal power, which denotes maximum tether tension, is reached at the centre point of the wind window(Azimuth ϕ equal to zero). The trajectory would therefore be much more powerful if it stays within the maximal power zone.

The best azimuth positioning of the trajectory appears to be a compromise between maximal power zone of the wind window and the vessel motion direction. Useful propulsive force within the wind window is presented in figure 5 for an apparent wind angle β_{WR} of 90 °, at 10 m. In a same manner, trajectory elevation can be adjusted to reach the best propulsive force level.

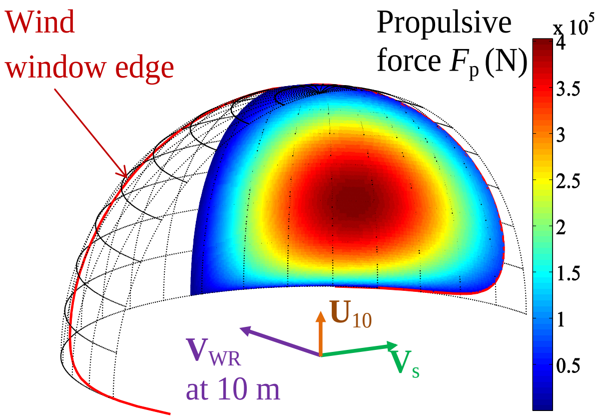

Figure 5: Propulsive force evolution within useful wind window for an β_{WR} angle of 90°.

The last control parameter which can be modified in the present study is the trajectory orientation. This parameter was added to the Naaijen et al. [10,11] approach to improve the dynamic flight performance of the kite. Indeed if an horizontal trajectory is usually more efficient in downwind condition, a trajectory parallel to the wind window edge (almost a vertical trajectory) would be much more efficient in upwind condition according to Dadd et al. [16]. Actually, a vertical trajectory close to the wind window edge allows a better positioning of the kite closer to the vessel course axis $\mathbf{x}_F$ in upwind condition. Moreover, in upwind condition the useful wind window is reduced, hence a vertical trajectory would fit much easier in the useful wind window in comparison with an horizontal trajectory.

4.4 OPTIMIZATION ALGORITHM

Based on vessel speed, true wind direction and velocity given at 10 m over sea level, an optimization algorithm is used to predict best kite flight conditions regarding propulsive force criterion. Results are expressed by maximal propulsive force polar plots. Thus, for each true wind angle β_{WT}, corresponding optimized flight configuration (either static or dynamic) was identified. In case of a static flight, the elevation corresponding to the best propulsive force was searched. Indeed, for a given elevation parameter, the azimuth angle ϕ leading to a positioning of the kite on the wind window edge could be indentified thanks to equation (13). A single-variable bounded nonlinear function minimization was used with Matlab® to find the best elevation. The maximal propulsive force generated by the kite in a static flight case, as defined in paragraph 3.4, could therefore be deduced. For the dynamic flight case, azimuth, elevation and trajectory orientation were optimized simultaneously to identify the most efficient trajectory regarding the average propulsive force. A multidimensional unconstrained nonlinear minimization (Nelder-Mead [19]) was used to find the best trajectory. Details about optimization strategy principle, previously done manually step by step for the study of a sailing yacht, are available in [20].

A comparison between static and dynamic flight propulsive forces led then to identify the best configuration. Additionally, this approach enables also the identification of drift (along $\mathbf{y}_F$) and vertical (along $\mathbf{z}_F$) force components.

5. RESULTS

5.1 INITIAL DATA

Kite parameters are similar to the case study of Dadd [12], in order to facilitate further comparisons.
Kite parameters are as follows:

- Kite Surface A_k: 320 m²
- Lift coefficient $C_{L:}$ 0.776
- Kite Lift to Drag Angle ε: 12.02 ° (lift to drag ratio 4.7)
- Tether length l_T: 300 m

Experimental conditions taken by Dadd [12]:

- Air density ρ_{air}: 1.19 kg.m^{-3}
- Wind velocity at 10 m U_{10}: 8.97 m.s^{-1} (17.5 kts)
- Vessel velocity V_s: 4.11 m.s^{-1} (8 kts)

The analytical expression of the 8-shaped trajectory is given by Wellicome and Wilkinson [8]. The size of the trajectory is the same as Dadd [12]:

- Azimuth amplitude: 66 °
- Elevation amplitude: 16 °

5.2 PROPULSIVE FORCE RESULTS

For each true wind angle β_{WT}, trajectory azimuth, elevation and orientation are optimized in the present algorithm. It can be seen in figure 6 that up to 50 ° static flight appears to be more efficient than dynamic flight. Indeed, in the case of a static flight, the kite is situated on the wind window edge as explained in paragraph 3.3. It corresponds to the closest position to the vessel motion axis $\mathbf{x}_F$ as shown in figure 5. Therefore, the static flight is more effective in upwind condition although it generates less tether tension than the dynamic flight.

Above 50 ° the best flight configuration is the dynamic one using vertical trajectories. Indeed, the closer the trajectory to the wind window edge is, the more efficient it will be as explained before. Moreover, vertical trajectories are easily contained in the useful wind window as explained in paragraph 4.3. Therefore, they are more efficient than horizontal trajectories in upwind conditions. Dadd obtained the same result in his work [12] while Naaijen et al. [10,11] obtained less propulsive force since he used only horizontal trajectories.

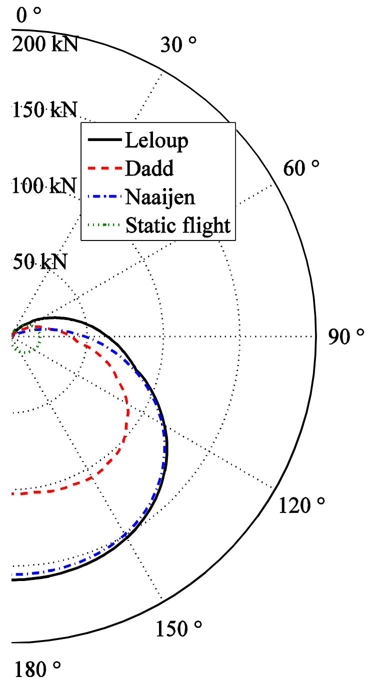

Figure 6: Optimal propulsive force using different trajectory optimization.

In upwind conditions, the drift force (along $\mathbf{y}_F$) can reach more than two times the propulsive force for a true wind angle of 90 °. Nevertheless, according to Naaijen et al. [10] the drift angle induced is less than 1 ° and the induced resistance is less than 1 %. A maximum drift angle of 3 ° and a maximum induced resistance of 4 %

were obtained in present study following the study of Brix [21] using a container ship whose manoeuvrability characteristics were taken from the work of Wolff [22]. Indeed, given the size of a merchant ship, the drift force remains negligible. However, in the case of a sailing yacht, the drift angle can be greater than 10 ° as presented in a previous work [20].

At a true wind angle of 109 °, the best 8-shaped trajectory becomes almost horizontal. The trajectory azimuth is calculated for each true wind angle in order to obtain the maximum propulsive force. For a true wind angle of 180 ° the maximum propulsive force is 159 kN as shown in figure 6.

Compared to those of Dadd [12] and Naaijen et al. [10,11], the present optimization process led to consistent results. Compared to Naaijen et al., and following Dadd, the present optimization demonstrates the major influence of the orientation, in tracking the optimal trajectory from upwind to downwind sailing conditions. Compared to Dadd, taking into account the precise wind gradient and wind window twist but also continuous variations of trajectory positioning parameters (instead of discrete sets of these parameters), improve noticeably the optimal result for each true wind angle.

5.3 FUEL SAVING VERSUS TRUE WIND ANGLE IN DIFFERENT WIND CONDITIONS.

***British Bombardier* characteristics**			
L_{WL}	Length water line	225.86	m
L_{oa}	Length over all	231.34	m
B	Beam	29.57	m
D	Draught	12.5	m
Δ	Displacement	66 716.225	t
S_h	Wetted area	10 105	m^2
C_t	Total resistance coefficient	0.002414	[-]
V_s	Ship service speed	15.5	kts
S_h	Wetted surface	10 108	m^2
P_B	Brake power of the engine (design)	12 000	kW
[-]	Number of propellers	1	[-]
D_{prop}	Propeller diameter	6.706	m
t	Thrust deduction factor	0.187	[-]
w	Wake factor	0.324	[-]
η_r	Relative rotative efficiency	0.99	[-]
η_{tr}	Transmission efficiency	0.97	[-]

Table 1: Vessel characteristics

To assess kite efficiency in term of fuel saving, the *British Bombardier* vessel, a 50 000 dwt tanker, presented by Naaijen et al. [10] was used in this study. The advantage of studying this ship is that all the necessary hydrodynamic data on the hull and engine are given in Naaijen et al. work [10] They are displayed in table 1. Indeed, knowing the ship speed, the total ship resistance can be calculated. The propulsive force given by the kite is subtracted from the total resistance of the ship R_T to obtain the force required from the propeller F_{prop}.

Taking into account the wake factor w and the thrust deduction factor t, the required propeller thrust T_{prop} can be calculated as a function of the advance velocity V_A at the propeller:

$$T_{prop} = \frac{c_1 V_A^2}{(1 - t)(1 - w)^2} = c_8 V_A^2 \tag{15}$$

Where the speed dependent factor c_1 is equal to:

$$c_1 = \frac{F_{prop}}{V_s^2} \tag{16}$$

And the advance velocity V_A at the propeller is obtained as a function of the wake factor:

$$V_A = V_s (1 - w) \tag{17}$$

Then the non-dimensional thrust coefficient K_T can be expressed by a quadratic function of the advance ratio J

$$K_T = \frac{T}{\rho_{water} D_p^4 n_{prop}^2} = \frac{c_8}{\rho_{water} D_p^2} J^2 \tag{18}$$

Where ρ_{water} is the water density (kg.m^{-3}),
D_p is the propeller diameter (m),
n_{prop} is number of revolution per second of the propeller,
J is advance ratio ($J = V_A / nD_p$).

Using the propeller open water diagram, the advance ratio J can be solved by matching the propeller open water K_T and the above deduced K_T. The number of propeller revolutions per second n is calculated from the expression of the advance ratio J. The corresponding torque coefficient K_Q is then obtained from the open water K_Q curve. Taking into account the relative rotative efficiency η_r and the transmission efficiency η_{tr}, the engine brake power P_B can be found as a function of torque Q_{prop}:

$$P_B = \frac{2\pi\, n_{prop}\, Q_{prop}}{\eta_r\, \eta_{tr}} = \frac{2\pi\, K_Q\, n_{prop}^3\, \rho_{water}\, D_p^5}{\eta_r\, \eta_{tr}} \tag{19}$$

The brake specific fuel consumption (BSFC in g.kWh^{-1}), which is given for the considered engine, is then calculated as a function of the normalized brake power P^*(which is a fraction of the nominal power):

$$BSFC = 43.53 (P^*)^2 – 78.111 (P^*) + 196.8 \tag{20}$$

Finally, the total fuel consumption is compared to the fuel consumption of the ship without kite propulsion assistance to obtain the instantaneous fuel saving provided by kite auxiliary propulsion. The kite is the same as the one presented in paragraph 5.1.

The trajectory size presented by Dadd et al. [12,16] was used but the analytical expression was taken from Argatov [17] since it was more convenient and it sped up the trajectory optimization process. Only the present optimization strategy, which appears to be the most effective, was used. The fuel saving was first computed for the Dadd’s case study [12] presented in paragraph 5.1 (V_s = 8 kts and U_{10} = 17.5 kts). As shown in figure 7, the fuel saving exceeds 5 % for a true wind direction of 68 ° thanks to vertical 8-shaped trajectories. It reaches 23.5 % downwind.

As a second step, the fuel saving was computed for a ship velocity of 15.5 kts which is the service speed of the *British Bombardier*. According to the literature [10,12], the true wind velocity was chosen to vary from 13.5 kts (4 Beaufort) to 30.5 kts (7 Beaufort). For a wind speed of 4 Beaufort the fuel saving using a kite as auxiliary propulsion system is less than 4 % as shown in figure 7. But for a wind speed of 5 Beaufort the fuel saving reaches 13.4 % for a true wind direction of 140 °. Then the more the wind velocity increases, the more the fuel saving increases. For a wind speed of 7 Beaufort, it exceeds 5 % for a true wind direction of 48 ° and it reaches 57 % in downwind condition. Finally, for the *British Bombardier* operation velocity of 15.5 kts, the use of a kite as auxiliary propulsion device becomes efficient for a true wind velocity of 5 Beaufort and the fuel savings could reach more than 50 % for a true wind velocity of 7 Beaufort. Nevertheless, this last result might be optimistic in real conditions, because a lot of parameters such as sea state and ship motions may significantly reduce savings.

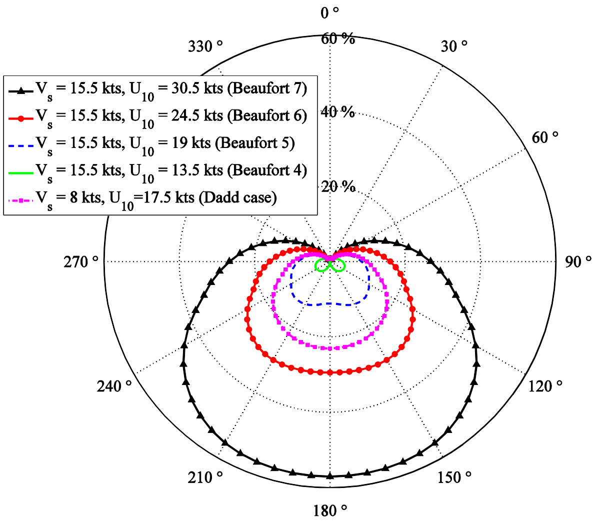

Figure 7: Fuel saving in different wind conditions and for different ship velocities.

5.4 VESSEL PERFORMANCE PREDICTION ON A GIVEN ROUTE.

The maritime route on the Atlantic Ocean between New-York and Cape Lizard shown in figure 8 was used to assess kite propulsion efficiency. The simulation was based on Grib data (true wind direction and magnitude at 10 m) recorded along the 5350 km route (2889 NM). The propulsive force provided by the kite was computed over the Atlantic sea crossing for a vessel speed of 15.5 kts.

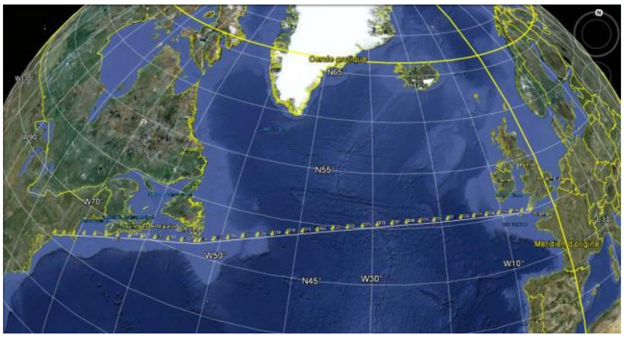

Figure 8: New York to Cape Lizard maritime route used for Grib data.

The propulsive force of the kite was computed every 148 km (80 NM) on the maritime route, assuming no wind changes between two points. Corresponding propulsive force stays constant between two points and results are shown in figure 9. On this route, the fuel saving generally stays between 5 % and 58 %. Kite efficiency decreases at the end of the route because of wind velocity reduction, hence apparent wind angle reduction. Nevertheless, despite upwind in that case, the trajectory optimization technique presented enables a positive kite propulsion force for such conditions. Finally, average fuel saving predicted is 26.6 %.

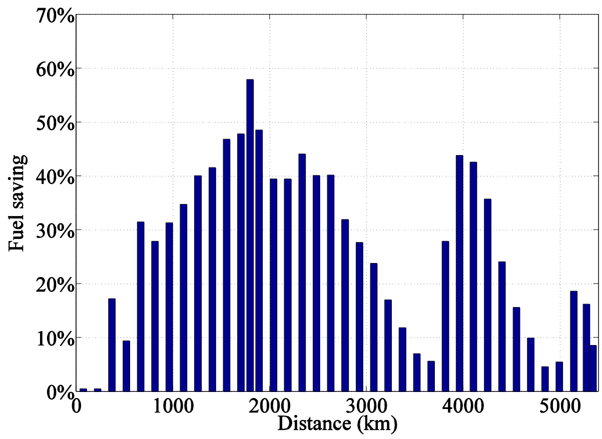

Figure 9: Fuel saving prediction on a New-York to Cape Lizard route.

6. CONCLUSION

A novel modelling for an analytical description of the kite motion is presented. The solving of the parameterization presented led to continuous kite velocities and tethers tensions predictions along the flight path within the wind window, including especially wind gradient and ship velocity. Both static and dynamic flight cases were considered regarding optimization strategy for kite tow efficiency. In the case of a dynamic flight, the trajectory orientation and its position within the wind window were optimized for each true wind angle. Magnitude orders of towing forces induced by the kite for static and dynamic flights were computed with the present optimization strategy and compared to those obtained with Dadd’s [12] and Naaijen et al. [10,11]

optimization strategies. It appears that the present optimization strategy enhances upwind capabilities on one hand and propulsive force for any wind conditions on the other hand. This is mainly due to the introduction of trajectory orientation and precise wind gradient but also to continuous optimization of trajectory parameters (instead of discrete sets of these parameters like Dadd [12]). A performance prediction program dedicated to a merchant ship was finally developed to assess fuel saving capabilities of a kite. The static flight has been also studied but it appears that it is efficient mainly for small wind angles. The static flight case would also ensure benefits for stronger wind conditions and vessel stability issues. In such cases, the use of kite static flights should avoid issues related to kite size change maneuvers which are weak points for kite towed systems.

The results presented are dependent on trajectory size. Nevertheless, the optimal trajectory size remains difficult to define. Indeed, it was experimentally observed that tethers tension and kite velocity decrease in turning stages at the extremities of an 8-shaped trajectory. This phenomenon was modelled in a simplified manner in a previous study [23], but this problem will still have to be addressed in future works to compute optimal trajectory size.

Furthermore, according to Naaijen et al. [10] and following the present study, the influence of drift seems to be negligible in the case of a merchant ship. The required rudder angle to obtain yaw balance is less than 3 ° [10]. Nevertheless, the impact of kite operating on ship manoeuvrability will have to be addressed more in details in the future. Indeed pitch and heave movements of the vessel have a considerable effect on kite tethers and on the kite itself. More detailed studies on the influence of pitch and heave movements will be useful to design damping systems to limit tension peaks in kite tethers.

Finally, these results are subjected to control command units that must be able to ensure reliable optimal flight trajectories. Required electrical supply for such control command units must still be estimated. Questions about woven fabrics durability and aerodynamic characteristics variations remain open ended.

7. ACKNOWLEDGEMENTS

The authors of this paper are grateful to the French ministry of defence and Yves Parlier for their financial support.

8. REFERENCES

1. LOYD, M.L., 'Crosswind Kite Power (for large-scale wind power production)'. *Journal of Energy, 4(3):106-111*, 1980.

2. DE GROOT, S.G.C., 'Modelling the dynamics of an arc-shaped kite for control law design'. *M. Sc. Thesis. Delft University of Technology*. 2010. URL (accessed July 2013): http://repository.tudelft.nl/view/ir/uuid%3A5f493a5d-da9c-457f-be28-799a63cb42d9/

3. TERINK, E., 'Kiteplane flight dynamics'. *M. Sc. Thesis, Delft University of Technology*. 2009.

4. FAGIANO, L., 'Control of tethered airfoils for high–altitude wind energy generation'. *Ph. D. Thesis. Royal Turin Polytechnic.* 2009. URL (accessed July 2013): http://lorenzofagiano.altervista.org/docs/PhD_thesis_Fagiano_Final.pdf

5. BREUKELS, J., 'An engineering methodology for kite design'. *Ph. D Thesis, Delft University of Technology,* 2011. URL (accessed July 2013): http://www.kitepower.eu/publications.html

6. MANEIA, G.M., 'Aerodynamic study of airfoils and wings for power kites applications'. *M. Sc. Thesis. Politecnico di Torino.* 2007. URL (accessed July 2013): http://maneia.com/doc/MasterThesisManeia.pdf

7. DE WACHTER, A., 'Kiteplane flight dynamics'. *M. Sc. Thesis, Delft University of Technology*. 2008.

8. WELLICOME, J.F., WILKINSON, S., 'Ship Propulsion Kites: An Initial Study'. *University of Southampton Department of Ship Science, Faculty of Engineering and Applied Science. Tech. Rept. SSSU 19*, 1984.

9. LELOUP, R., RONCIN, K., BLES, G., LEROUX, J.B., JOCHUM, C., PARLIER, Y., 'Estimation of the lift-to-drag ratio using the lifting line method: application to a Leading Edge Inflatable kite'. *In: Ahrens U, Diehl M, Schmehl R (Eds.). Airborne Wind Energy. Springer*. ch. 18, 2013.

10. NAAIJEN, P., KOSTER, V., DALLINGA, R.P., 'On the power savings by an auxiliary kite propulsion system. *International shipbuilding progress', 53(4): 255-279*, 2006.

11. NAAIJEN, P., SHI, W., KHERIAN, J.G., 'Assessing the fuel saving by using auxiliary wind propulsion from traction kites. Ship design and operation for environmental sustainability', *In: Ship design and operation for environmental sustainability, The royal institution of naval architects (RINA), London*, 2010.

12. DADD, G.M., 'Kite dynamics for ship propulsion'. *Ph. D. Thesis. University of Southampton*. 2013.

13. ERHARD, M., STRAUCH, H., 'Control of towing kites for seagoing vessels'. 2012. arXiv:1202.3641v1.URL(accessed July 2013): http://arxiv.org/pdf/1202.3641.pdf

14. COSTELLO, S., FRANCOIS, G., BONVIN, D., 'Real-Time Optimization for Kites'. *In: 5th IFAC International Workshop on Periodic Control Systems (PSYCO'2013).* 2013.

15. DADD, G.M., HUDSON, D.A., SHENOI, R.A., 'Comparison of two kite force models with experiment'. *Journal of Aircraft, 47(1):212-224*, 2010.

16. DADD, G.M., HUDSON, D.A., SHENOI, R.A., 'Determination of kite forces using three-dimensional flight trajectories for ship propulsion'. *Renewable Energy, 36(10): 2667-2678*, 2011.

17. ARGATOV, I., RAUTAKORPI, P., SILVENNOINEN, R., 'Estimation of the mechanical energy output of the kite wind generator'. *Renewable Energy, vol. 34, no 6, p. 1525-1532*, 2009.

18. 'ITTC Symbols and Terminology List'. *International Towing Tank Conference.* Version 2011.

19. NELDER, J.A., MEAD, R.A., 'Simplex method for function minimization'. *The computer journal, 7(4): 308-313*, 1965.

20. LELOUP, R., RONCIN, K., BLES, G., LEROUX, J.B., JOCHUM, C., PARLIER, Y., 'Kite and classical rig sailing performance comparison on a one design keel boat'. *In: Third International Conference on Innovation in High Performance Sailing Yachts, Lorient, France*. 2013.

21. BRIX, J., 'Manoeuvring Technical Manual', *Seehafen Verlag*, 1993.

22. WOLFF, K., 'Ermittlung der Manövriereigenschaften fünf repräsentativer. Schiffstypen mit Hilfe von CPMC-Modellversuchen', *Report 412 of Institut für Schiffbau Hamburg*, 1981

23. LELOUP, R., RONCIN, K., BLES, G., LEROUX, J.B., JOCHUM, C., PARLIER, Y., 'Estimation of the effect of rotation on the drag angle by using the lifting line method: application to towing kites for auxiliary propulsion of vessels'. *In: 13[èmes] Journées de l'Hydrodynamique. Chatou. France.* 2012. URL (accessed July 2013): http://website.ec-nantes.fr/actesjh/images/13JH/Annexe/13jh-s04.htm

9. AUTHORS BIOGRAPHY

Richard Leloup is currently following a Ph.D. Degree at the graduate and post graduate school of engineering, Ecole Nationale Supérieure de Techniques Avancées Bretagne (ENSTA Bretagne), Brest, Brittany, France. He graduated at ENSTA Bretagne in 2011 in naval architecture and offshore engineering. He is a member of the team which was launched in 2011 to work closely with the French sailor Yves Parlier on his "Beyond the Sea" project. His research focuses on modelling approaches and computational tools for kites sails kinematics and strengthening issues.

Kostia Roncin is Associate Professor of Naval Hydrodynamics at the graduate and post graduate school of engineering, Ecole Nationale Supérieure de Techniques Avancées Bretagne (ENSTA Bretagne), Brest, Brittany, France. He is currently the head of the Master of Science in Naval Hydrodynamics and gave during several years specialized lectures in naval construction and design. He received his Ph.D. degree (2000) with Honours from the University of Nantes, France. His research skills cover seakeeping, manoeuvrability and sail yacht dynamics.

Guilhem Bles is Associate Professor of Mechanical Engineering and Materials Science at the graduate and post graduate school of engineering, Ecole Nationale Supérieure de Techniques Avancées Bretagne (ENSTA Bretagne), Brest, Brittany, France. He is currently in charge of Naval and Offshore design courses. He received his Ph.D. degree (2002) with Honours from the University of Grenoble, France. His research skills cover woven fabrics and polymeric materials constitutive behaviours at large strain transformations.

Jean-Baptiste Leroux is Associate Professor of Naval Hydrodynamics at the graduate and post graduate school of engineering, Ecole Nationale Supérieure de Techniques Avancées Bretagne (ENSTA Bretagne), Brest, Brittany, France. He is currently in charge of fluid mechanics courses. He received his Ph.D. degree (2003) with Honours from the University of Nantes, France. His research skills mainly cover cavitation and hydrodynamics instabilities.

Christian Jochum is Associate Professor of Mechanical Engineering and Materials Science at the graduate and post graduate school of engineering, Ecole Nationale Supérieure de Techniques Avancées Bretagne (ENSTA Bretagne), Brest, Brittany, France. He worked several years in the Industry as head of the research department for a French supplier of track maintenance and construction equipment, involved in rigid body mechanics and structures design. He received his Ph.D. degree (1999) with Honours from the University of Metz, Lorraine, France. His research skills cover thermosetting composites from multiphysics couplings and internal stress issues to dynamical behaviour and strengthening.

Yves Parlier has succeeded brilliantly in all the major nautical races and has strived throughout his life to promote respect for man and the environment. He has a graduate degree in composite materials and launched several innovations in sail yacht design. We remember the Vendée Globe 2000 when all alone, near an island off New Zealand, he successfully rebuilt and erected a new mast and finished his voyage around the world. Taking advantage of wind energy by using kites as auxiliary propulsion device is the aim of the “Beyond the sea” project launched by Yves Parlier.